Hardware and Spectrum Sharing for Distributed Massive MIMO

Andrea P. Guevara, Cheng-Ming Chen, Sofie Pollin
Department of Electrical Engineering, KU Leuven, Belgium
Email:{aguevara,cchen,spollin}@esat.kuleuven.be

***Abstract*—Massive MIMO promises unprecedented spectral efficiency as values exceeding 140 b/s/Hz have already been demonstrated in the lab for a single cell. In this paper, based on measurements obtained in a distributed Massive MIMO testbed, we compare the spectral efficiency, area spectral efficiency, and capacity of two adjacent cells under different levels of cooperation and the impact of co-channel interference. This is the first Massive MIMO measurement based analysis of the performance of spectrum and infrastructure sharing, showing that in fully cooperative systems (sharing infrastructure and spectrum) there is an improvement of the area spectral efficiency by 50% and a sixfold of capacity in comparison with a scenario without sharing, i.e. conventional two-cells planning. In comparison to the scenario where only spectrum is shared, the infrastructure and spectrum sharing case also increases the area spectral efficiency by two and the overall capacity by four. In addition, the use of M-MMSE increases the performance of the system in 43% in relation to RZF, for this particular scenario when co-channel interference is considered.**

***Index Terms*—Infrastructure sharing, Massive MIMO, spectral efficiency, spectrum sharing.**

I. Introduction

As the number of wireless users will increase in the near future, solutions that enable to share the same frequency resources in space are becoming more important. Massive MIMO is considered one of the best Radio Access Network (RAN) candidates in 5G. In Massive MIMO a large number of antennas is deployed in a Base Station (BS) that is capable of coherently serving multiple users at the same time and frequency resource.

The use of a large number of antennas in a BS enables high spatial multiplexing, which increases the spectral efficiency and capacity of the system [1]. In addition, it is believed that inter-cell interference vanishes when the array size increases. However, in reality, array sizes are finite and there are also important correlations between the channels seen by the users in adjacent cells.

The location of the antennas also impacts the system performance. In Massive MIMO, two main topologies, i.e., distributed and collocated antenna arrays have been broadly studied in [2]–[5]. The advantages of a distributed Massive MIMO deployment include the increase in coverage area, possibility to exploit diversity, and decreased shadowing effect. On the other hand, using distributed massive MIMO imposes strict backhaul and synchronization requirements, a coherent processing of the received signals at the multiple distributed subarrays, and, on top of that, a high capital expenditure in infrastructure deployment in a large number of sites.

From the economic point of view, infrastructure sharing is one of the possible solutions to reduce operating expenses (OPEX) and capital expenses (CAPEX). In an infrastructure sharing scenario, two or more operators lend their own or third-party network resources to other operators under different level agreements. This cooperation method has been shown to result in a high improvement of the profits of all stakeholders involved [6]. So, in this scenario, numerous Base Stations (BSs) are shared between several operators over dedicated or common frequencies. For a full level of infrastructure and spectrum cooperation, there is not only monetary reward but also an increase in the performance of the system as it is shown in [7], where authors demonstrated valuable insights about the sharing approaches through simulations of resource sharing in mmWave networks.

Unlike [7], the aim of this paper is to contrast Spectral Efficiency (SE), area SE and capacity of three Massive MIMO scenarios under different levels of infrastructure and spectrum sharing, with multiple combining vectors. We rely on a real up-link (UL) measured channel, which was collected in an outdoor distributed experiment using KULeuven Massive MIMO testbed.

The paper is organized as follows: Section II describes our system model and a set of multiple combining vectors given in the literature, and how they are related with the spectral efficiency and capacity of the system. Section III describes the experiment carried out to obtain the results discussed in Section IV. To finalize, Section V draws the main conclusions.

The following notation is used throughout the paper: $\mathbf{x} \in \mathbb{C}^{\mathrm{M}}$ represents an [M×1] complex vector, $\mathbf{X} \in \mathbb{C}^{[\mathrm{M}\times\mathrm{N}]}$ is an [M×N] complex matrix. $\mathbf{x}^{\mathrm{H}}$ and $\mathbf{x}^{\mathrm{T}}$ states a transpose and conjugate-transpose of vector $\mathbf{x}$.

II. System model and spectral efficiency

In the following section the system model is presented, followed by a compendium of different combining vectors and the metrics used to compare the performance of different systems.

A. System Model

In this work, a multi-cell Time Divison Duplex (TDD) Massive MIMO system is considered. This system has L cells, each of them has M antennas deployed in one BSs, and K

single antenna users per cell. The transmission power from user k in cell j is p_{jk} and the wireless link or channel vector between the same user and all the antennas deployed in BS in cell l is $\mathbf{h}_{jk}^{l}$, with a path gain β_{jk}^{l}.

B. Channel estimation

During uplink training, each user first sends a sequence of orthogonal pilots (τ_p) over its channel to the BS. As all users send their pilots at the same time, the BS receives a signal which contains information of all the user channels. Once this training signal reaches the BS, it is decorrelated using the conjugate pilots of each user, then all the estimated channels ($\hat{\mathbf{h}}_{jk}^{l}$) are obtained in the BS l[1]. Thus, the channel estimation matrix from all users in cell j to a BS in cell l is $\hat{\mathbf{H}}_{j}^{l} = [\hat{\mathbf{h}}_{j1}^{l} ... \hat{\mathbf{h}}_{jK}^{l}]$.

From the channel estimation procedure a covariance matrix error $\mathbf{C}_{jk}^{l}$ is obtained as:

$$\mathbf{C}_{jk}^{l} = \mathbb{E}\left\{\tilde{\mathbf{h}}_{jk}^{l}\left(\tilde{\mathbf{h}}_{jk}^{l}\right)^{\mathrm{H}}\right\}, \tag{1}$$

where $\tilde{\mathbf{h}}_{jk}^{l}$ is the channel error, and it is the difference between the ideal channel and its estimated channel: $\tilde{\mathbf{h}}_{jk}^{l} = \mathbf{h}_{jk}^{l} - \hat{\mathbf{h}}_{jk}^{l}$.

C. Combining vectors

Once channel estimation is completed, the UL data transmission can start. Assuming that the desired signal (s_{jk}) is the data transmitted from user k in cell j to the BS in cell j, the UL received signal is:

$$\mathbf{y}_j = \hat{\mathbf{h}}_{jk}^{j} s_{jk} + \sum_{l=1}^{L} \sum_{\substack{i=1 \\ (l,i)\neq(j,k)}}^{K} \hat{\mathbf{h}}_{il}^{j} s_{il} + \mathbf{n}. \tag{2}$$

The first term of Eq. (2) is the desired signal over the estimated channel, the second term is inter- and intra-cell interference, and the last term is noise $\mathbf{n} \sim \mathcal{CN}(\mathbf{0}, \sigma_{\mathrm{UL}}^{2}\mathbf{I})$.

To obtain the desired signal while suppressing interference and noise, BS j uses a combining vector matrix for all users in cell j as $\mathbf{V}_j = [\mathbf{v}_{j1} ... \mathbf{v}_{jK}]$.

Multiple combining vectors have been proposed in the state-of-the-art [8]. These rely on different channel information to coherently combine the desired signal, this information could be: channel estimation error, intra-cell information, or intra- and inter-cell information, as described below:

- *Maximum Ratio Combining (MRC)* uses only the estimated channel matrix within the analyzed cell j to maximize all desired signals:

$$\mathbf{V}^{\mathrm{MR}} = \hat{\mathbf{H}}_{j}^{j}. \tag{3}$$

  This combining vector is one of the most used due to its low computational complexity.
- *Zero-Forcing (ZF)* detection cancels all intra-cell interference as:

$$\mathbf{V}^{\mathrm{ZF}} = \hat{\mathbf{H}}_{j}^{j}\left(\left(\hat{\mathbf{H}}_{j}^{j}\right)^{\mathrm{H}}\hat{\mathbf{H}}_{j}^{j}\right)^{-1}, \tag{4}$$

  thus only the desired signal will remain. This combining vector is suitable when all users have high SNR.
- *Regularized Zero-Forcing (ZF)* receive combining makes a trade-off between suppressing the intra-cell interference or the noise, based on the estimated channel matrix with a regularized diagonal matrix: $\sigma_{\mathrm{UL}}^{2}\mathbf{P}_{j}^{-1}$. It can be expressed as:

$$\mathbf{V}^{\mathrm{RZF}} = \hat{\mathbf{H}}_{j}^{j}\left(\left(\hat{\mathbf{H}}_{j}^{j}\right)^{\mathrm{H}}\hat{\mathbf{H}}_{j}^{j} + \sigma_{\mathrm{UL}}^{2}\mathbf{P}_{j}^{-1}\right)^{-1}, \tag{5}$$

  where $\mathbf{P}_j = \mathrm{diag}(p_{j1} ... p_{jk})$.
- *Minimum-Mean Squared Error (MMSE)* in Eq. (6) uses a whitened process to detect the desired data with the aid of channel estimation statistics, minimizing the noise and interference from the received signal

$$\mathbf{V}_{j}^{\mathrm{MMSE}} = \left(\hat{\mathbf{H}}_{j}^{j}\mathbf{P}_{j}\left(\hat{\mathbf{H}}_{j}^{j}\right)^{\mathrm{H}} + \sum_{i=1}^{K} p_{ji}\mathbf{C}_{ji}^{j} + \eta + \sigma_{\mathrm{UL}}^{2}\mathbf{I}_{M_j}\right)^{-1}\hat{\mathbf{H}}_{j}^{j}\mathbf{P}_{j}. \tag{6}$$

  MMSE has two variations: a first variant is Single-cell MMMSE (S-MMSE) which uses only intra-cell interference, for this case $\eta = 0$ in (6). A second variant is Multi-cell MMSE (M-MMSE) which considers both inter- and intra-cell interference. M-MMSE is recognized as the optimal scheme, for this case η in Eq. (6) is:

$$\eta = \sum_{\substack{l=1 \\ l\neq j}}^{L} \hat{\mathbf{H}}_{l}^{j}\mathbf{P}_{l}\left(\hat{\mathbf{H}}_{l}^{j}\right)^{\mathrm{H}} + \sum_{\substack{l=1 \\ l\neq j}}^{L}\sum_{i=1}^{K} p_{li}\mathbf{C}_{li}^{j}. \tag{7}$$

D. Network performance metrics

To quantify the performance of a system in different scenarios and under different combining vectors, this paper propose three metrics: SE, area SE and capacity.

The instantaneous SE per user is used to compute the amount of UL data per Hz received successfully at the BS. Considering that MMSE channel estimation is used in this work, the lower bound of the channel capacity for user k in cell j can be expressed as Theorem 4.1 in [8]:

$$\mathrm{SE}_{jk} = \frac{\tau_u}{\tau_c}\,\mathbb{E}\left\{\log_2\left(1 + \gamma_{jk}^{\mathrm{UL}}\right)\right\} \quad [\mathrm{bits/s/Hz}]. \tag{8}$$

In the expression above, γ_{jk} is the signal-to-interference-plus-noise ratio (SINR) of the analyzed user and can be expressed as:

$$\gamma_{jk} = \frac{p_{jk}|\mathbf{v}_{jk}^{\mathrm{H}}\hat{\mathbf{h}}_{jk}^{j}|^2}{\sum_{l=1}^{L}\sum_{\substack{i=1 \\ (l,i)\neq(j,k)}}^{K} p_{li}|\mathbf{v}_{jk}^{\mathrm{H}}\hat{\mathbf{h}}_{li}^{j}|^2 + \mathbf{v}_{jk}^{\mathrm{H}}\left(\sum_{l=1}^{L}\sum_{i=1}^{K} p_{li}\mathbf{C}_{li}^{j} + \sigma_{\mathrm{UL}}^{2}\mathbf{I}_{M_j}\right)\mathbf{v}_{jk}}, \tag{9}$$

where $\mathbf{v}_{jk}$ is any of the combining vector schemes presented in Section II-C and τ_u/τ_c is the portion of coherence block used to transmit UL data.

[1]For a detailed explanation of pilot allocation and channel estimation refer to Section 3.1 and Section 3.2 in [8].

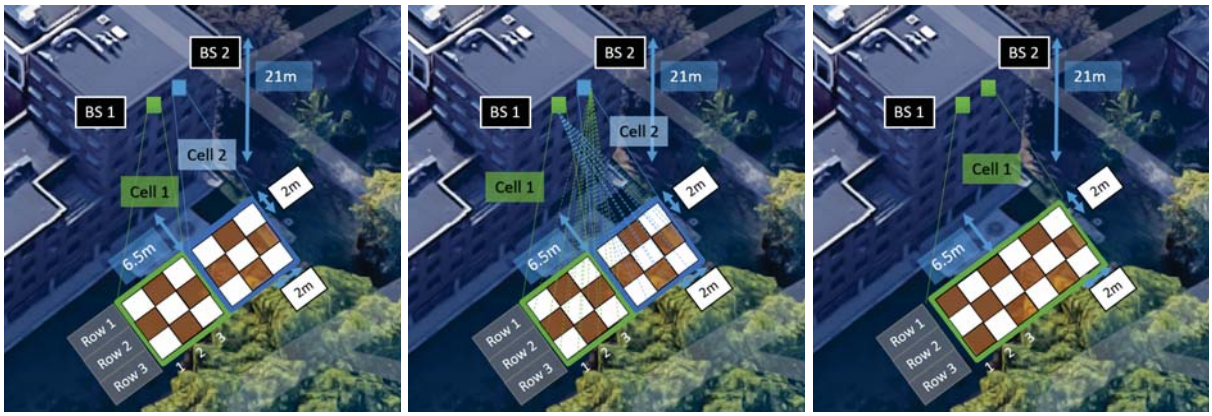

(a) Two-cells scenario: Each cell operates in a different band centered on different carrier frequency without interference.

(b) Spectrum sharing scenario: Both cells operates in the same band without coordinated spectrum sharing.

(c) Infrastructure and spectrum sharing scenario: Two coordinated BSs serve all UEs in the system, using the same band.

Fig. 1: Overlook of the symmetric two-cell outdoor scenario at ESAT KU Leuven. The location of each BS is 21 meters high and separated by 6.5 meters. Each cell supports 18 UEs distributed in 3 rows and 6 columns grid area.

For the sake of a fair comparison between heterogeneous cells of varying size, we use area SE. Therefore for a cell j with area A_j:

$$\mathrm{ASE}_j = \frac{1}{A_j} \sum_{k=1}^{K} \mathrm{SE}_{jk} \quad [\mathrm{bits/s/Hz/m^2}]. \tag{10}$$

The last performance metric considered in this paper is capacity C, which is the number of uplink bits successfully transmitted over a period of time in a given bandwidth. So, for a cell j which uses bandwidth BW_j, the capacity is:

$$\mathrm{C}_j = \mathrm{BW}_j \sum_{k=1}^{K} \mathrm{SE}_{jk} \quad [\mathrm{bits/s}]. \tag{11}$$

III. Massive MIMO experiment

A description of the outdoor experiment that was carried out with the KULeuven Massive MIMO testbed is detailed in this section, followed by an explanation of how the data is selected for different scenarios.

A. Measurement campaign

For this experiment, we used the Massive MIMO testbed based on LTE-TDD, set at 2.6 GHz center frequency and bandwidth of 20 MHz, described in detail in [12]. This testbed has two main components, the first one is the BS which has 64-antennas, as a unique feature, those antennas are equally distributed in two patch arrays. All 64-antennas are connected by pairs to 32 Universal Software Radio Peripherals (USRPs). The system runs in LabVIEW Communications MIMO Application Framework 1.1 [13]. The second component of this testbed consists of the users, which are deployed in pairs on a single USRP. Each user is equipped with a dipole antenna which is attached to an external power amplifier (13 dBm) additional to the USPR's internal amplifier (20 dBm).

Both antenna arrays were located on the sixth floor of KULeuven ESAT building at 21 m above the ground level. Those arrays were separated by a distance of 6.5 m and located at the rear windows of the mentioned building, with 24^{o} of inclination from the floor. In the case of the users, a single USRP was sequentially placed on different locations on the ground floor with a direct Line-of-Sight (LOS) to both antenna arrays. As we can see in Fig. 1, the single USRP which run a pair of users was deployed in a grid area of 18 locations, each location had 2 m in both length and width. For each USRP's location, the uplink channel was collected in both antenna arrays.

B. Virtual scenarios

The channel data collected from the experiment described above was first processed offline, setting each user's SNR between 30 dB and 38 dB. Then, the system SE was calculated by computing the combining vectors according to the following scenarios:

- Two-cells scenario: A common cellular planing of two-cells is considered, in which 18 users are served by one antenna array. Let us assume that each cell works at different carrier frequency and has 10 MHz bandwidth, thus for this case there is no inter-cell interference, Fig. 1a.
- Spectrum sharing scenario: Similar to the previous scenario, one array serves as a virtual cell to 18 users, however, for this case, we assume that both cells operate at the same frequency with a combined bandwidth of 20 MHz under uncoordinated spectrum sharing. Therefore, inter-cell interference will impact the performance of each cell, Fig. 1b.
- Spectrum and infrastructure sharing scenario: In this case, we consider two cells that are perfectly synchronized, then inter-cell interference is removed. This scenario is

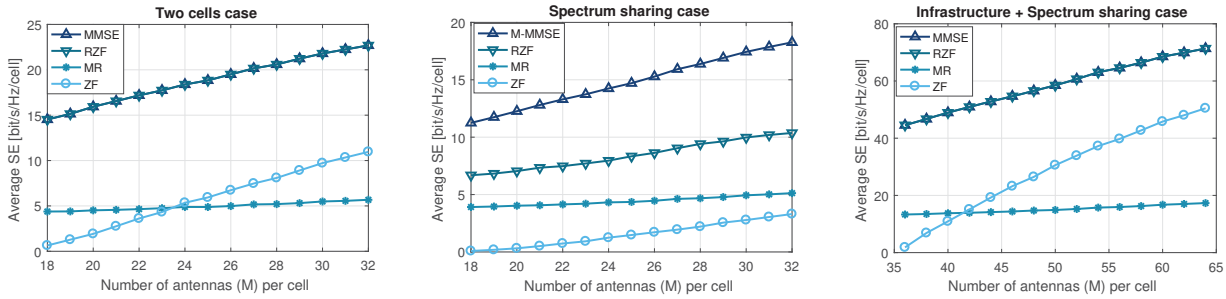

(a) The average SE per cell in a system with two independent cells, that operateon different carrier frequencies.

(b) The average SE per cell in a two-cell system with a shared carrier frequency and co-channel interference.

(c) SE in a system with distributed BS, where two networks share spectrum and infrastructure

Fig. 2: Average spectral efficiency per cell versus number of active antennas, under different types of combining vectors in a system with 36 users.

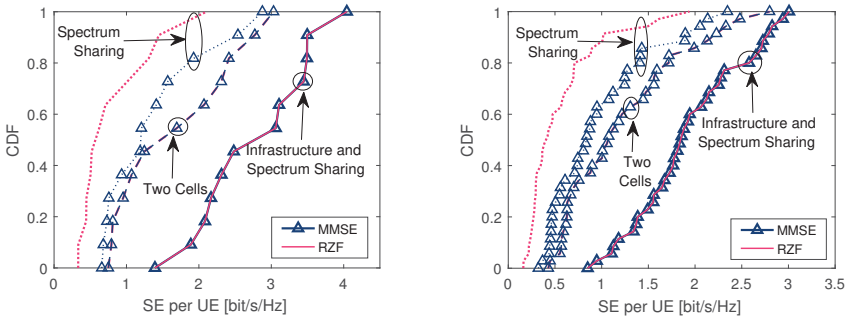

(a) SE CDF per user when 12 users in the whole system are active.

(b) SE CDF per user when 36 users in the whole system are active

Fig. 3: CDF comparison of SE per UE for all scenarios by MMSE and RZF combining vectors, when M = 64.

also considered as a distributed massive MIMO system where two base stations cooperate with each other serving all the users simultaneously with a total bandwidth of 20 MHz, Fig. 1c.

IV. Numerical Results

In this section, we present the numerical results evaluated in each virtual scenario, contrasting three network performance metrics: spectrum efficiency, area spectrum efficiency and capacity.

A. Spectral efficiency and combining vectors.

Combining vector selection influences the SINR and SE performance as it is shown in Fig. 2. In this set of figures, the average SE per cell is obtained against varying numbers of active antennas per cell when $K \leq M$ and under different combining vectors: MMSE, RZF, ZF and MR. In general, the SE increases as the number of antennas grows, regardless of the combining vector selected.

SE per cell is the highest when MMSE and RZF are selected in scenarios without inter-cell interference, as seen in Fig. 2a and 2c. Those values are similar because the SNR per user has high value and there is no pilot contamination, therefore, the channel estimation does not influence the SE.

Notice in Fig. 2b that each cell is affected by inter-cell interference, in this case η in M-MMSE (Eq. 6) contains information of the neighboring cell which helps to maximize the SINR and SE in contrast with RZF. Although M-MMSE boosts the SE in this case, spectrum sharing shows the worst performance with respect to the other scenarios.

Undoubtedly, the case with the best SE per cell is shown in Fig 2c when not only the spectrum is shared but also the infrastructure. Its main advantage is the absence of inter-cell interference as both distributed antenna arrays are synchronized. Interestingly, we can see that when M is not bigger than K, ZF can not decorrelate the signals from all users effectively, therefore, it has a lower performance than MR (see Fig. 1a when $M < 24$ and in Fig. 2c when $M < 42$).

B. SE cumulative distribution function (CDF).

An evaluation of the SE per user using the CDF is presented in Fig. 3, showing a comparison of all the scenarios using RZF and MMSE combining vectors under different number of active users. In Fig. 3a only users in row 3 of Fig. 1 are considered while in Fig. 3b all users are active. From this two

Scenario	Area per cell [m^2]	Bandwidth per cell [MHz]	SE [bits/s/Hz/cell]		Area SE [bits/s/Hz/m^2]		Capacity [Mbits/s]	
			RZF	MMSE	RZF	MMSE	RZF	MMSE
Two-cell	36	10	22.69		0.63		226.9	
Spectrum sharing	26	20	10.37	18.23	0.288	0.506	207.4	364.4
Infrastructure + spectrum sharing	72	20	71.36		0.991		1427.2	

TABLE I: Network performance metrics for all the study scenarios, with all active antennas and all users.

figures, we can see that when the number of users is small, the SE per user increases due to the reduction of intra-cell interference.

Similarly to the SE per cell results, the infrastructure and spectrum sharing strategy maximizes SE per UE, regardless of the number of active users. In addition, this case shows the gain that M-MMSE ($\gamma_l \neq 0$) has over RZF in a realistic multi-cell scenario for 12 and 36 active users.

C. SE, area SE and Capacity.

Table I shows a numerical comparison between the network performance metrics presented in Section II-D when all antennas and users are active. The SE per cell was analyzed previously under different numbers of users and combining vectors. However, due to different cell sizes across the scenarios, the area SE provides a more fair comparison between different scenarios.

For all the metrics, spectrum and infrastructure sharing case provides the best performance as a system. Improving area SE by approximately 50% in comparison with the two-cells case, and almost 100% more for spectrum sharing case when M-MMSE is applied. Following the same trend, an infrastructure and shared scenario increases the capacity six times more than a two-cells case and about four times to the highest achievable value (M-MMSE) for spectrum share case.

For spectrum sharing scenario, inter-cell interference is suppressed with M-MMSE increasing all parameters performance by 43% in comparisons with RZF. Surprisingly, the capacity of the spectrum sharing case surpasses the two-cells scenario only when M-MMSE is used.

V. Conclusions

Based on a distributed massive MIMO measurement campaign, this work has provided three main conclusions for systems with multiple levels of cooperation. First, a fully cooperative system which shares infrastructure and spectrum is capable of achieving up to 50% more area spectral efficiency in comparison with a non-cooperative one (two-cells scenario); infrastructure and spectrum sharing case also increases around twice the value of area spectral efficiency in a system which only shares spectrum (spectrum sharing scenario). Second, the system capacity of infrastructure and spectrum sharing scenario increase a fourfold in relation with a spectrum sharing case and a sixfold for a two-cells case. Third, to improve all the aforementioned network parameters, the selection of a combining vector is essential: when M-MMSE is implemented, it achieves 43% higher spectrum efficiency, area spectrum efficiency and capacity as it minimizes co-channel interference.

Acknowledgment

This work was funded by the European Union's Horizon 2020 under grant agreement no. 732174 (ORCA project).

References

[1] Larsson, E. G., Edfors, O., Tufvesson, F., and Marzetta, T. L. (2014). Massive MIMO for next generation wireless systems. IEEE communications magazine, 52(2), 186-195.

[2] Liu, Z., and Dai, L. (2014). A Comparative Study of Downlink MIMO Cellular Networks With Co-Located and Distributed Base-Station Antennas. IEEE Trans. Wireless Communications, 13(11), 6259-6274.

[3] Wang, J., and Dai, L. (2015). Asymptotic rate analysis of downlink multi-user systems with co-located and distributed antennas. IEEE Transactions on Wireless Communications, 14(6), 3046-3058.

[4] Kamga, G. N., Xia, M., and Aïssa, S. (2016). Spectral-efficiency analysis of massive MIMO systems in centralized and distributed schemes. IEEE Transactions on Communications, 64(5), 1930-1941. Resource Sharing in 5G mmWave Cellular Networks.

[5] C. Chen, V. Volskiy, A. Chiumento, L. Van der Perre, G. A. E. Vandenbosch and S. Pollin. (2016). Exploration of User Separation Capabilities by Distributed Large Antenna Arrays, 2016 IEEE Globecom Workshops (GC Wkshps).

[6] T. Frisanco, P. Tafertshofer, P. Lurin and R. Ang, "Infrastructure sharing and shared operations for mobile network operators From a deployment and operations view," NOMS 2008 - 2008 IEEE Network Operations and Management Symposium, Salvador, Bahia, 2008, pp. 129-136.

[7] Rebato, M., Mezzavilla, M., Rangan, S., and Zorzi, M. (2016). Resource sharing in 5G mmWave cellular networks. 2016 IEEE Conference on Computer Communications Workshops (INFOCOM WKSHPS), 271-276.

[8] E. Bjornson, J. Hoydis , and L. Sanguinetti (2017), "Massive MIMO Networks: Spectral, Energy, and Hardware Efficiency", Foundations and Trends in Signal Processing: pp. 154-655.

[9] Li, C., Zhang, J., and Letaief, K. B. (2014). Throughput and energy efficiency analysis of small cell networks with multi-antenna base stations. IEEE Transactions on Wireless Communications, 13(5), 2505-2517.

[10] D. Cao, S. Zhou and Z. Niu, "Optimal base station density for energy-efficient heterogeneous cellular networks," 2012 IEEE International Conference on Communications (ICC), Ottawa, ON, 2012, pp. 4379-4383.

[11] Wu, Y., Louie, R. H., McKay, M. R., and Collings, I. B. (2012). Generalized framework for the analysis of linear MIMO transmission schemes in decentralized wireless ad hoc networks. IEEE Transactions on Wireless Communications, 11(8), 2815-2827.

[12] Chen, C. M., Volski, V., Van der Perre, L., Vandenbosch, G. A., and Pollin, S. (2017). Finite large antenna arrays for Massive MIMO: characterisation and system impact. IEEE Transactions on Antennas and Propagation.

[13] National Instruments. (2017). "5G Massive MIMO Testbed: From Theory to Reality (white paper)", http://www.ni.com/white-paper/52382/en/